1.10

DENSITY-FUNCTIONAL PERTURBATION THEORY

Paolo Giannozzi[1] and Stefano Baroni[2]
[1]*DEMOCRITOS-INFM, Scuola Normale Superiore, Pisa, Italy*
[2]*DEMOCRITOS-INFM, SISSA-ISAS, Trieste, Italy*

The calculation of vibrational properties of materials from their electronic structure is an important goal for materials modeling. A wide variety of physical properties of materials depend on their lattice-dynamical behavior: specific heats, thermal expansion, and heat conduction; phenomena related to the electron–phonon interaction such as the resistivity of metals, superconductivity, and the temperature dependence of optical spectra, are just a few of them. Moreover, vibrational spectroscopy is a very important tool for the characterization of materials. Vibrational frequencies are routinely and accurately measured mainly using infrared and Raman spectroscopy, as well as inelastic neutron scattering. The resulting vibrational spectra are a sensitive probe of the local bonding and chemical structure. Accurate calculations of frequencies and displacement patterns can thus yield a wealth of information on the atomic and electronic structure of materials.

In the Born–Oppenheimer (adiabatic) approximation, the nuclear motion is determined by the nuclear Hamiltonian $\mathcal{H}$:

$$\mathcal{H} = -\sum_I \frac{\hbar^2}{2M_I}\frac{\partial^2}{\partial \mathbf{R}_I^2} + E(\{\mathbf{R}\}), \tag{1}$$

where $\mathbf{R}_I$ is the coordinate of the Ith nucleus, M_I its mass, $\{\mathbf{R}\}$ indicates the set of all the nuclear coordinates, and $E(\{\mathbf{R}\})$ is the ground-state energy of the Hamiltonian, $H_{\{\mathbf{R}\}}$, of a system of N interacting electrons moving in the field of fixed nuclei with coordinates $\{\mathbf{R}\}$:

$$H_{\{\mathbf{R}\}} = -\frac{\hbar^2}{2m}\sum_i \frac{\partial^2}{\partial \mathbf{r}_i^2} + \frac{e^2}{2}\sum_{i\neq j}\frac{1}{|\mathbf{r}_i - \mathbf{r}_j|} + \sum_{i,I} v_I(\mathbf{r}_i - \mathbf{R}_I) + E_N(\{\mathbf{R}\}), \tag{2}$$

S. Yip (ed.),
Handbook of Materials Modeling, 195–214.

where $\mathbf{r}_i$ is the coordinate of the ith electron, m is the electron mass, $-e$ is the electron charge, $E_N(\{\mathbf{R}\})$ is the nuclear electrostatic energy:

$$E_N(\{\mathbf{R}\}) = \frac{e^2}{2} \sum_{I \neq J} \frac{Z_I Z_J}{|\mathbf{R}_I - \mathbf{R}_J|}, \tag{3}$$

Z_I being the charge of the Ith nucleus, and v_I is the electron–nucleus Coulomb interaction: $v_I(\mathbf{r}) = -Z_I e^2/r$. In a pseudopotential scheme each nucleus is thought to be lumped together with its own core electrons in a frozen ion which interacts with the valence electrons through a smooth pseudopotential, $v_I(\mathbf{r})$.

The equilibrium geometry of the system is determined by the condition that the forces acting on all nuclei vanish. The forces $\mathbf{F}_I$ can be calculated by applying the Hellmann–Feynman theorem to the Born–Oppenheimer Hamiltonian $H_{\{\mathbf{R}\}}$:

$$\mathbf{F}_I \equiv -\frac{\partial E(\{\mathbf{R}\})}{\partial \mathbf{R}_I} = -\left\langle \Psi_{\{\mathbf{R}\}} \left| \frac{\partial H_{\{\mathbf{R}\}}}{\partial \mathbf{R}_I} \right| \Psi_{\{\mathbf{R}\}} \right\rangle, \tag{4}$$

where $\Psi_{\{\mathbf{R}\}}(\mathbf{r}_1, \ldots, \mathbf{r}_N)$ is the ground-state wavefunction of the electronic Hamiltonian, $H_{\{\mathbf{R}\}}$. Eq. (4) can be rewritten as:

$$\mathbf{F}_I = -\int n(\mathbf{r}) \frac{\partial v_I(\mathbf{r} - \mathbf{R}_I)}{\partial \mathbf{R}_I} \mathrm{d}\mathbf{r} - \frac{\partial E_N(\{\mathbf{R}\})}{\partial \mathbf{R}_I}, \tag{5}$$

where $n(\mathbf{r})$ is the electron charge density for the nuclear configuration $\{\mathbf{R}\}$:

$$n(\mathbf{r}) = N \int |\Psi_{\{\mathbf{R}\}}(\mathbf{r}, \mathbf{r}_2, \ldots, \mathbf{r}_N)|^2 \mathrm{d}\mathbf{r}_2 \cdots \mathrm{d}\mathbf{r}_N. \tag{6}$$

For a system near its equilibrium geometry, the harmonic approximation applies and the nuclear Hamiltonian of Eq. (1) reduces the Hamiltonian of a system of independent harmonic oscillators, called *normal modes*. Normal mode frequencies, ω, and displacement patterns, U_I^α for the αth Cartesian component of the Ith atom, are determined by the secular equation:

$$\sum_{J,\beta} \left(C_{IJ}^{\alpha\beta} - M_I \omega^2 \delta_{IJ} \delta_{\alpha\beta} \right) U_J^\beta = 0, \tag{7}$$

where $C_{IJ}^{\alpha\beta}$ is the matrix of *interatomic force constants* (IFCs):

$$C_{IJ}^{\alpha\beta} \equiv \frac{\partial^2 E(\{\mathbf{R}\})}{\partial R_I^\alpha \partial R_J^\beta} = -\frac{\partial F_I^\alpha}{\partial R_J^\beta}. \tag{8}$$

Various dynamical models, based on empirical or semiempirical inter-atomic potentials, can be used to calculate the IFCs. In most cases, the parameters of the model are obtained from a fit to some known experimental data, such as a set of frequencies. Although simple and often effective, such approaches tend

to have a limited predictive power beyond the range of cases included in the fitting procedure. It is often desirable to resort to first-principles methods, such as density-functional theory, that have a far better predictive power even in the absence of any experimental input.

1. Density-Functional Theory

Within the framework of density-functional theory (DFT), the energy $E(\{\mathbf{R}\})$ can be seen as the minimum of a *functional* of the charge density $n(\mathbf{r})$:

$$E(\{\mathbf{R}\}) = T_0[n(\mathbf{r})] + \frac{e^2}{2}\int \frac{n(\mathbf{r})n(\mathbf{r}')}{|\mathbf{r}-\mathbf{r}'|}\,\mathrm{d}\mathbf{r}\,\mathrm{d}\mathbf{r}' + E_{\mathrm{xc}}[n(\mathbf{r})] + \int V_{\{\mathbf{R}\}}(\mathbf{r})n(\mathbf{r})\mathrm{d}\mathbf{r} + E_N(\{\mathbf{R}\}), \tag{9}$$

with the constrain that the integral of $n(\mathbf{r})$ equals the number of electrons in the system, N. In Eq. (9), $V_{\{\mathbf{R}\}}$ indicates the external potential acting on the electrons, $V_{\{\mathbf{R}\}} = \sum_I v_I(\mathbf{r}-\mathbf{R}_I)$, $T_0[n(\mathbf{r})]$ is the kinetic energy of a system of *noninteracting* electrons having $n(\mathbf{r})$ as ground-state density,

$$T_0[n(\mathbf{r})] = -2\frac{\hbar^2}{2m}\sum_{n=1}^{N/2}\int \psi_n^*(\mathbf{r})\frac{\partial^2\psi_n(\mathbf{r})}{\partial\mathbf{r}^2}\,\mathrm{d}\mathbf{r} \tag{10}$$

$$n(\mathbf{r}) = 2\sum_{n=1}^{N/2}|\psi_n(\mathbf{r})|^2, \tag{11}$$

and E_{xc} is the so-called *exchange-correlation energy*. For notational simplicity, the system is supposed here to be a nonmagnetic insulator, so that each of the $N/2$ lowest-lying orbital states accommodates two electrons of opposite spin. The Kohn-Sham (KS) orbitals are the solutions of the KS equation:

$$H_{\mathrm{SCF}}\psi_n(\mathbf{r}) \equiv \left(-\frac{\hbar^2}{2m}\frac{\partial^2}{\partial\mathbf{r}^2} + V_{\mathrm{SCF}}(\mathbf{r})\right)\psi_n(\mathbf{r}) = \epsilon_n\psi_n(\mathbf{r}), \tag{12}$$

where H_{SCF} is the Hamiltonian for an electron under an effective potential V_{SCF}:

$$V_{\mathrm{SCF}}(\mathbf{r}) = V_{\{\mathbf{R}\}}(\mathbf{r}) + e^2\int\frac{n(\mathbf{r}')}{|\mathbf{r}-\mathbf{r}'|}\,\mathrm{d}\mathbf{r}' + v_{\mathrm{xc}}(\mathbf{r}), \tag{13}$$

and v_{xc} – the *exchange-correlation potential* – is the functional derivative of the exchange-correlation energy: $v_{\mathrm{xc}}(\mathbf{r}) \equiv \delta E_{\mathrm{xc}}/\delta n(\mathbf{r})$. The form of E_{xc} is unknown: the entire procedure is useful only if reliable approximate expressions for E_{xc} are available. It turns out that even the simplest of such expressions, the local-density approximation (LDA), is surprisingly good in many

cases, at least for the determination of electronic and structural ground-state properties. Well-established methods for the solution of KS equations, Eq. (12), in both finite (molecules, clusters) and infinite (crystals) systems, are described in the literature. The use of more sophisticated and more performing functionals than LDA (such as generalized gradient approximation, or GGA) is now widespread.

An important consequence of the variational character of DFT is that the Hellmann–Feynman form for forces, Eq. (5), is still valid in a DFT framework. In fact, the DFT expression for forces contains a term coming from explicit derivation of the energy functional $E(\{\mathbf{R}\})$ with respect to atomic positions, plus a term coming from implicit dependence via the derivative of the charge density:

$$\mathbf{F}_I^{\mathrm{DFT}} = -\int n(\mathbf{r}) \frac{\partial V_{\{\mathbf{R}\}}(\mathbf{r})}{\partial \mathbf{R}_I}\,\mathrm{d}\mathbf{r} - \frac{\partial E_N(\{\mathbf{R}\})}{\partial \mathbf{R}_I} - \int \frac{\delta E(\{\mathbf{R}\})}{\delta n(\mathbf{r})} \frac{\partial n(\mathbf{r})}{\partial \mathbf{R}_I}\,\mathrm{d}\mathbf{r}. \quad (14)$$

The last term in Eq. (14) vanishes exactly for the ground-state charge density: the minimum condition implies in fact that the functional derivative of $E(\{\mathbf{R}\})$ equals a constant – the Lagrange multiplier that enforces the constrain on the total number of electrons – and the integral of the derivative of the electron density is zero because of charge conservation. As a consequence, $\mathbf{F}_I^{\mathrm{DFT}} = \mathbf{F}_I$ as in Eq. (5). Forces in DFT can thus be calculated from the knowledge of the electron charge-density.

IFCs can be calculated as finite differences of Hellmann–Feynman forces for small finite displacements of atoms around the equilibrium positions. For finite systems (molecules, clusters) this technique is straightforward, but it may also be used in solid-state physics (*frozen phonon* technique). An alternative technique is the direct calculation of IFCs using density-functional perturbation theory (DFPT) [1–3].

2. Density-Functional Perturbation Theory

An explicit expression for the IFCs can be obtained by differentiating the forces with respect to nuclear coordinates, as in Eq. (8):

$$\frac{\partial^2 E(\{\mathbf{R}\})}{\partial \mathbf{R}_I \partial \mathbf{R}_J} = \int \frac{\partial n(\mathbf{r})}{\partial \mathbf{R}_J} \frac{\partial V_{\{\mathbf{R}\}}(\mathbf{r})}{\partial \mathbf{R}_I}\mathrm{d}\mathbf{r} + \delta_{IJ}\int n(\mathbf{r}) \frac{\partial^2 V_{\{\mathbf{R}\}}(\mathbf{r})}{\partial \mathbf{R}_I \partial \mathbf{R}_J}\mathrm{d}\mathbf{r} + \frac{\partial^2 E_N(\{\mathbf{R}\})}{\partial \mathbf{R}_I \partial \mathbf{R}_J}. \quad (15)$$

The calculation of the IFCs thus requires the knowledge of the ground-state charge density, $n(\mathbf{r})$, as well as of its linear response to a distortion of the nuclear geometry, $\partial n(\mathbf{r})/\partial \mathbf{R}_I$.

The charge-density linear response can be evaluated by linearizing Eqs. (11)–(13), with respect to derivatives of KS orbitals, density, and potential, respectively. Linearization of Eq. (11) leads to:

$$\frac{\partial n(\mathbf{r})}{\partial \mathbf{R}_I} = 4\,\mathrm{Re}\sum_{n=1}^{N/2} \psi_n^*(\mathbf{r})\frac{\partial \psi_n(\mathbf{r})}{\partial \mathbf{R}_I}. \tag{16}$$

Whenever the unperturbed Hamiltonian is time-reversal invariant, eigenfunctions are either real, or they occur in conjugate pairs, so that the prescription to keep only the real part in the above formula can be dropped. The derivatives of the KS orbitals, $\partial\psi_n(\mathbf{r})/\partial\mathbf{R}_I$, are obtained from linearization of Eqs. (12) and (13):

$$(H_{\mathrm{SCF}} - \epsilon_n)\frac{\partial \psi_n(\mathbf{r})}{\partial \mathbf{R}_I} = -\left(\frac{\partial V_{\mathrm{SCF}}(\mathbf{r})}{\partial \mathbf{R}_I} - \frac{\partial \epsilon_n}{\partial \mathbf{R}_I}\right)\psi_n(\mathbf{r}), \tag{17}$$

where

$$\frac{\partial V_{\mathrm{SCF}}(\mathbf{r})}{\partial \mathbf{R}_I} = \frac{\partial V_{\{\mathbf{R}\}}(\mathbf{r})}{\partial \mathbf{R}_I} + e^2\int \frac{1}{|\mathbf{r}-\mathbf{r}'|}\frac{\partial n(\mathbf{r}')}{\partial \mathbf{R}_I}\mathrm{d}\mathbf{r}' + \int \frac{\delta v_{xc}(\mathbf{r})}{\delta n(\mathbf{r}')}\frac{\partial n(\mathbf{r}')}{\partial \mathbf{R}_I}\mathrm{d}\mathbf{r}' \tag{18}$$

is the first-order derivative of the self-consistent potential, and

$$\frac{\partial \epsilon_n}{\partial \mathbf{R}_I} = \left\langle \psi_n \left| \frac{\partial V_{\mathrm{SCF}}}{\partial \mathbf{R}_I} \right| \psi_n \right\rangle \tag{19}$$

is the first-order derivative of the KS eigenvalue, ϵ_n. The form of the right-hand side of Eq. (17) ensures that $\partial\psi_n(\mathbf{r})/\partial\mathbf{R}_I$ can be chosen so as to have a vanishing component along $\psi_n(\mathbf{r})$ and thus the singularity of the linear system in Eq. (17) can be ignored.

Equations (16)–(18) form a set of self-consistent linear equations. The linear system, Eq. (17), can be solved for each of the $N/2$ derivatives $\partial\psi_n(\mathbf{r})/\partial\mathbf{R}_I$ separately, the charge-density response calculated from Eq. (16), and the potential response $\partial V_{\mathrm{SCF}}/\partial\mathbf{R}_I$ is updated from Eq. (18), until self-consistency is achieved. Only the knowledge of the occupied states of the system is needed to construct the right-hand side of the equation, and efficient iterative algorithms – such as conjugate gradient or minimal residual methods – can be used for the solution of the linear system. In the atomic physics literature, an equation analogous to Eq. (17) is known as the Sternheimer equation, and its self-consistent version was used to calculate atomic polarizabilities. Similar methods are known in the quantum chemistry literature, under the name of *coupled Hartree–Fock* method for the Hartree–Fock approximation [4, 5].

The connection with standard first-order perturbation (linear-response) theory can be established by expressing Eq. (17) as a sum over the spectrum of the unperturbed Hamiltonian:

$$\frac{\partial \psi_n(\mathbf{r})}{\partial \mathbf{R}_I} = \sum_{m \neq n} \psi_m(\mathbf{r}) \frac{1}{\epsilon_n - \epsilon_m} \left\langle \psi_m \left| \frac{\partial V_{\rm SCF}}{\partial \mathbf{R}_I} \right| \psi_n \right\rangle, \tag{20}$$

running over all the states of the system, occupied and empty. Using Eq. (20), the electron charge-density linear response, Eq. (16), can be recast into the form:

$$\frac{\partial \psi_n(\mathbf{r})}{\partial \mathbf{R}_I} = 4 \sum_{n=1}^{N/2} \sum_{m \neq n} \psi_n^*(\mathbf{r}) \psi_m(\mathbf{r}) \frac{1}{\epsilon_n - \epsilon_m} \left\langle \psi_m \left| \frac{\partial V_{\rm SCF}}{\partial \mathbf{R}_I} \right| \psi_n \right\rangle. \tag{21}$$

This equations shows that the contributions to the electron-density response coming from products of occupied states cancel each other. As a consequence, in Eq. (17) the derivatives $\partial \psi_n(\mathbf{r})/\partial \mathbf{R}_I$ can be assumed to be orthogonal to all states of the occupied manifold.

An alternative and equivalent point of view is obtained by inserting Eq. (16) into Eq. (18) and the resulting equation into Eq. (17). The set of $N/2$ self-consistent linear systems is thus recast into a single huge linear system for all the $N/2$ derivatives $\partial \psi_n(\mathbf{r})/\partial \mathbf{R}_I$

$$(H_{\rm SCF} - \epsilon_n) \frac{\partial \psi_n(\mathbf{r})}{\partial \mathbf{R}_I} + \sum_{m=1}^{N/2} \left(K_{nm} \frac{\partial \psi_m}{\partial \mathbf{R}_I} \right) (\mathbf{r}) = -\frac{\partial V_{\{\mathbf{R}\}}(\mathbf{r})}{\partial \mathbf{R}_I} \psi_n(\mathbf{r}), \tag{22}$$

under the orthogonality constraints:

$$\left\langle \psi_n \left| \frac{\partial \psi_n}{\partial \mathbf{R}_I} \right\rangle \right. = 0. \tag{23}$$

The nonlocal operator K_{nm} is defined as:

$$\left(K_{nm} \frac{\partial \psi_m}{\partial \mathbf{R}_I} \right) (\mathbf{r}) = 4 \int \psi_n(\mathbf{r}) \left(\frac{e^2}{|\mathbf{r} - \mathbf{r}'|} + \frac{\delta v_{\rm xc}(\mathbf{r})}{\delta n(\mathbf{r}')} \right) \psi_m^*(\mathbf{r}') \frac{\partial \psi_m}{\partial \mathbf{R}_I}(\mathbf{r}') \, {\rm d}\mathbf{r}'. \tag{24}$$

The same expression can be derived from a variational principle. The energy functional, Eq. (9), is written in terms of the perturbing potential and of the perturbed KS orbitals:

$$V^{(u_I)} \simeq V_{\{\mathbf{R}\}}(\mathbf{r}) + u_I \frac{\partial V_{\{\mathbf{R}\}}(\mathbf{r})}{\partial \mathbf{R}_I}, \quad \psi_n^{(u_I)} \simeq \psi_n(\mathbf{r}) + u_I \frac{\partial \psi_n(\mathbf{r})}{\partial \mathbf{R}_I}, \tag{25}$$

and expanded up to second order in the strength u_I of the perturbation. The first-order term gives the Hellmann–Feynman forces. The second-order one is a quadratic functional in the $\partial \psi_n(\mathbf{r})/\partial \mathbf{R}_I$s whose minimization yields

Eq. (22). This approach forms the basis of variational DFPT [6, 7], in which all the IFCs are expressed as minima of suitable functionals. The big linear system of Eq. (22) can be directly solved with iterative methods, yielding a solution that is perfectly equivalent to the self-consistent solution of the smaller linear systems of Eq. (17). The choice between the two approaches is thus a matter of computational strategy.

3. Phonon Modes in Crystals

In perfect crystalline solids, the position of the Ith atom can be written as:

$$\mathbf{R}_I = \mathbf{R}_l + \boldsymbol{\tau}_s = l_1\mathbf{a}_1 + l_2\mathbf{a}_2 + l_3\mathbf{a}_3 + \boldsymbol{\tau}_s \tag{26}$$

where $\mathbf{R}_l$ is the position of the lth unit cell in the Bravais lattice and $\boldsymbol{\tau}_s$ is the equilibrium position of the sth atom in the unit cell. $\mathbf{R}_l$ can be expressed as a sum of the three primitive translation vectors $\mathbf{a}_1, \mathbf{a}_2, \mathbf{a}_3$, with integer coefficients l_1, l_2, l_3. The electronic states are classified by a wave-vector $\mathbf{k}$ and a band index ν:

$$\psi_n(\mathbf{r}) \equiv \psi_{\nu,\mathbf{k}}(\mathbf{r}), \qquad \psi_{\nu,\mathbf{k}}(\mathbf{r}+\mathbf{R}_l) = e^{i\mathbf{k}\cdot\mathbf{R}_l}\psi_{\nu,\mathbf{k}}(\mathbf{r}) \quad \forall l, \tag{27}$$

where $\mathbf{k}$ is in the first Brillouin zone, i.e.: the unit cell of the *reciprocal lattice*, defined as the set of all vectors $\{\mathbf{G}\}$ such that $\mathbf{G}_l \cdot \mathbf{R}_m = 2\pi n$, with n an integer number.

Normal modes in crystals (*phonons*) are also classified by a wave-vector $\mathbf{q}$ and a mode index ν. Phonon frequencies, $\omega(\mathbf{q})$, and displacement patterns, $U_s^\alpha(\mathbf{q})$, are determined by the secular equation:

$$\sum_{t,\beta} \left(\tilde{C}_{st}^{\alpha\beta}(\mathbf{q}) - M_s\omega^2(\mathbf{q})\delta_{st}\delta_{\alpha\beta} \right) U_t^\beta(\mathbf{q}) = 0. \tag{28}$$

The *dynamical matrix*, $\tilde{C}_{st}^{\alpha\beta}(\mathbf{q})$, is the Fourier transform of real-space IFCs:

$$\tilde{C}_{st}^{\alpha\beta}(\mathbf{q}) = \sum_l e^{-i\mathbf{q}\cdot\mathbf{R}_l} C_{st}^{\alpha\beta}(\mathbf{R}_l). \tag{29}$$

The latter are defined as

$$C_{st}^{\alpha\beta}(l,m) \equiv \frac{\partial^2 E}{\partial u_s^\alpha(l)\partial u_t^\beta(m)} = C_{st}^{\alpha\beta}(\mathbf{R}_l - \mathbf{R}_m), \tag{30}$$

where $\mathbf{u}_s(l)$ is the deviation from the equilibrium position of atom s in the lth unit cell:

$$\mathbf{R}_I = \mathbf{R}_l + \boldsymbol{\tau}_s + \mathbf{u}_s(l). \tag{31}$$

Because of translational invariance, the real-space IFCs, Eq. (30), depend on l and m only through the difference $\mathbf{R}_l - \mathbf{R}_m$. The derivatives are evaluated

at $\mathbf{u}_s(l) = 0$ for all the atoms. The direct calculation of such derivatives in an infinite periodic system is however not possible, since the displacement of a single atom would break the translational symmetry of the system.

The elements of the dynamical matrix, Eq. (29), can be written as second derivatives of the energy with respect to a lattice distortion of wave-vector $\mathbf{q}$:

$$\tilde{C}_{st}^{\alpha\beta}(\mathbf{q}) = \frac{1}{N_\mathrm{c}} \frac{\partial^2 E}{\partial u_s^{*\alpha}(\mathbf{q}) \partial u_t^{\beta}(\mathbf{q})}, \tag{32}$$

where N_c is the number of unit cells in the crystal, and $\mathbf{u}_s(\mathbf{q})$ is the amplitude of the lattice distortion:

$$\mathbf{u}_s(l) = \mathbf{u}_s(\mathbf{q}) e^{i\mathbf{q}\cdot\mathbf{R}_l}. \tag{33}$$

In the frozen-phonon approach, the calculation of the dynamical matrix at a generic point of the Brillouin zone presents the additional difficulty that a crystal with a small distortion, Eq. (33), "frozen-in," loses the original periodicity, unless $\mathbf{q} = 0$. As a consequence, an enlarged unit cell, called *supercell*, is required for the calculation of IFCs at any $\mathbf{q} \neq 0$. The suitable supercell for a perturbation of wave-vector $\mathbf{q}$ must be big enough to accommodate $\mathbf{q}$ as one of the reciprocal-lattice vectors. Since the computational effort needed to determine the forces (i.e., the electronic states) grows approximately as the cube of the supercell size, the frozen-phonon method is in practice limited to lattice distortions that do not increase the unit cell size by more than a small factor, or to lattice-periodical ($\mathbf{q} = 0$) phonons.

The dynamical matrix, Eq. (32), can be decomposed into an electronic and an ionic contribution:

$$\tilde{C}_{st}^{\alpha\beta}(\mathbf{q}) = {}^{\mathrm{el}}\tilde{C}_{st}^{\alpha\beta}(\mathbf{q}) + {}^{\mathrm{ion}}\tilde{C}_{st}^{\alpha\beta}(\mathbf{q}), \tag{34}$$

where:

$$\begin{aligned} {}^{\mathrm{el}}\tilde{C}_{st}^{\alpha\beta}(\mathbf{q}) = \frac{1}{N_\mathrm{c}} \Bigg[& \int \left(\frac{\partial n(\mathbf{r})}{\partial u_s^{\alpha}(\mathbf{q})} \right)^* \frac{\partial V_{\{\mathbf{R}\}}(\mathbf{r})}{\partial u_t^{\beta}(\mathbf{q})} \, \mathrm{d}\mathbf{r} \\ & + \delta_{st} \int n(r) \frac{\partial^2 V_{\{\mathbf{R}\}}(\mathbf{r})}{\partial u_s^{*\alpha}(\mathbf{q}=0) \partial u_t^{\beta}(\mathbf{q}=0)} \, \mathrm{d}r \Bigg]. \end{aligned} \tag{35}$$

The ionic contribution – the last term in Eq. (15) – comes from the derivatives of the nuclear electrostatic energy, Eq. (3), and does not depend on the electronic structure. The second term in Eq. (34) depends only on the charge density of the unperturbed system and it is easy to evaluate. The first term in Eq. (34) depends on the charge-density linear response to the lattice distortion of Eq. (33), corresponding to a perturbing potential characterized by a single wave-vector $\mathbf{q}$:

$$\frac{\partial V_{\{\mathbf{R}\}}(\mathbf{r})}{\partial \mathbf{u}_s(\mathbf{q})} = -\sum_l \frac{\partial v_s(\mathbf{r} - \mathbf{R}_l - \boldsymbol{\tau}_s)}{\partial \mathbf{r}} e^{i\mathbf{q}\cdot\mathbf{R}_l}. \tag{36}$$

An advantage of DFPT with respect to the frozen-phonon technique is that the linear response to a monochromatic perturbation is also monochromatic with the same wave-vector $\mathbf{q}$. This is a consequence of the linearity of DFPT equations with respect to the perturbing potential, especially evident in Eq. (22). The calculation of the dynamical matrix can thus be performed for any $\mathbf{q}-$vector without introducing supercells: the dependence on $\mathbf{q}$ factors out and all the calculations can be performed on lattice-periodic functions. Real-space IFCs can then be obtained via discrete (fast) Fourier transforms. To this end, dynamical matrices are first calculated on a uniform grid of $\mathbf{q}$-vectors in the Brillouin zone:

$$\mathbf{q}_{l_1,l_2,l_3} = l_1 \frac{\mathbf{b}_1}{N_1} + l_2 \frac{\mathbf{b}_2}{N_2} + l_3 \frac{\mathbf{b}_3}{N_3}, \tag{37}$$

where $\mathbf{b}_1, \mathbf{b}_2, \mathbf{b}_3$ are the primitive translation vectors of the reciprocal lattice, l_1, l_2, l_3 are integers running from 0 to $N_1 - 1$, $N_2 - 1$, $N_3 - 1$, respectively. A discrete Fourier transform produces the IFCs in real space: $\tilde{C}_{st}^{\alpha\beta}(\mathbf{q}_{l_1,l_2,l_3}) \rightarrow C_{st}^{\alpha\beta}(\mathbf{R}_{l_1,l_2,l_3})$, where the real-space grid contains all $\mathbf{R}-$vectors inside a supercell, whose primitive translation vectors are $N_1\mathbf{a}_1$, $N_2\mathbf{a}_2$, $N_3\mathbf{a}_3$:

$$\mathbf{R}_{l_1,l_2,l_3} = l_1\mathbf{a}_1 + l_2\mathbf{a}_2 + l_3\mathbf{a}_3. \tag{38}$$

Once this has been done, the IFCs thus obtained can be used to calculate inexpensively via (inverse) Fourier transform dynamical matrices at any $\mathbf{q}$ vector not included in the original reciprocal-space mesh. This procedure is known as *Fourier interpolation*. The number of dynamical matrix calculations to be performed, $N_1N_2N_3$, is related to the range of the IFCs in real space: the real-space grid must be big enough to yield negligible values for the IFCs at the boundary vectors. In simple crystals, this goal is typically achieved for relatively small values of N_1, N_2, N_3 [8, 9]. For instance, the phonon dispersions of Si and Ge shown in Fig. 1 were obtained with $N_1 = N_2 = N_3 = 4$.

4. Phonons and Macroscopic Electric Fields

Phonons in the long-wavelength limit ($\mathbf{q} \rightarrow 0$) may be associated with a macroscopic polarization, and thus a homogeneous electric field, due to the long-range character of the Coulomb forces. The splitting between longitudinal optic (LO) and transverse optic (TO) modes at $\mathbf{q} = 0$ for simple polar semiconductors (e.g., GaAs), and the absence of LO–TO splitting in nonpolar semiconductors (e.g., Si), is a textbook example of the consequences of such phenomenon.

Macroscopic electrostatics in extended systems is a tricky subject from the standpoint of microscopic *ab initio* theory. In fact, on the one hand, the macroscopic polarization of an extended system depends on surface effects; on the

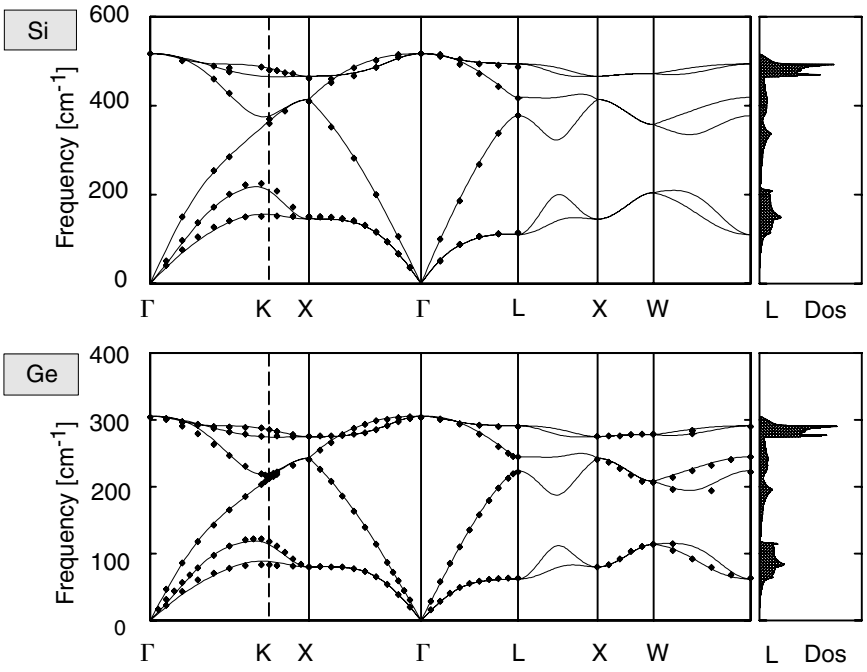

Figure 1. Calculated phonon dispersions and density of states for crystalline Si and Ge. Experimental data are denoted by diamonds. Reproduced from Ref. [8].

other hand, the potential which generates a homogeneous electric field is both nonperiodic and not bounded from below: an unpleasant situation when doing calculations using Born–von Kármán periodic boundary conditions. In the last decade, the whole field has been revolutionized by the advent of the so called *modern theory of electric polarization* [10, 11]. From the point of view of lattice dynamics, a more traditional approach based on perturbation theory is however appropriate because all the pathologies of macroscopic electrostatics disappear in the linear regime, and the polarization response to a homogeneous electric field and/or to a periodic lattice distortion – which is all one needs in order to calculate long-wavelength phonon modes – is perfectly well-defined.

In the long-wavelength limit, the most general expression of the energy as a quadratic function of atomic displacements, $\mathbf{u}_s(\mathbf{q}=0)$ for atom s, and of a macroscopic electric field, $\mathbf{E}$, is:

$$E(\{\mathbf{u}\},\mathbf{E}) = \frac{1}{2}\sum_{st}\sum_{\alpha\beta}\mathbf{u}_s\cdot{}^{\mathrm{an}}\tilde{\mathbf{C}}_{st}\cdot\mathbf{u}_t - \frac{\Omega}{8\pi}\mathbf{E}\cdot\boldsymbol{\epsilon}_\infty\cdot\mathbf{E} - e\sum_s\mathbf{u_s}\cdot\mathbf{Z}^\star_s\cdot\mathbf{E}, \tag{39}$$

where Ω is the volume of the unit cell; ϵ^{∞} is the electronic (i.e., clamped nuclei) dielectric tensor of the crystal; $\mathbf{Z}_s^{\star}$ is the tensor of *Born effective charges* [12] for atom s; and ${}^{\mathrm{an}}\tilde{\mathbf{C}}$ is the $\mathbf{q}=0$ dynamical matrix of the system, calculated at vanishing macroscopic electric field. Because of Maxwell's equations, the polarization induced by a longitudinal phonon in the $\mathbf{q} \to 0$ limit generates a macroscopic electric field which exerts a force on the atoms, thus affecting the phonon frequency. This, in a nutshell, is the physical origin of the LO–TO splitting in polar materials. Minimizing Eq. (39) with respect to the electric field amplitude at fixed lattice distortion yields an expression for the energy which depends on atomic displacements only, defining an effective dynamical matrix which contains an additional ("nonanalytic") contribution:

$$\tilde{C}_{st}^{\alpha\beta} = {}^{\mathrm{an}}\tilde{C}_{st}^{\alpha\beta} + {}^{\mathrm{na}}\tilde{C}_{st}^{\alpha\beta}, \tag{40}$$

where

$${}^{\mathrm{na}}\tilde{C}_{st}^{\alpha\beta} = \frac{4\pi e^2}{\Omega} \frac{\sum_{\gamma} Z_s^{\star\gamma\alpha} q_{\gamma} \sum_{\nu} Z_t^{\star\nu\beta} q_{\nu}}{\sum_{\gamma,\nu} q_{\gamma} \epsilon_{\infty}^{\gamma\nu} q_{\nu}} = \frac{4\pi e^2}{\Omega} \frac{(\mathbf{q} \cdot \mathbf{Z}_s^{\star})_{\alpha} \, (\mathbf{q} \cdot \mathbf{Z}_t^{\star})_{\beta}}{\mathbf{q} \cdot \boldsymbol{\epsilon}^{\infty} \cdot \mathbf{q}} \tag{41}$$

displays a nonanalytic behavior in the limit $\mathbf{q} \to 0$. As a consequence, the resulting IFCs are long-range in real space, with a dependence on the interatomic distance, which is typical of the dipole–dipole interaction. Because of this long-range behavior, the Fourier technique described above must be modified: a suitably chosen function of $\mathbf{q}$, whose $q \to 0$ limit is the same as in Eq. (41), is subtracted from the dynamical matrix in $\mathbf{q}$-space. This procedure makes residual IFCs short-range and suitable for Fourier transform on a relatively small grid of points. The nonanalytic term previously subtracted out in $\mathbf{q}$-space is then readded in real space. An example of application of such procedure is shown in Fig. 2, for phonon dispersions of some III–VI semiconductors.

The link between the phenomenological parameters $Z^{\star}$ and ϵ_{∞} of Eq. (39) and their microscopic expression is provided by conventional electrostatics. From Eq. (39) we obtain the expression for the electric induction $\mathbf{D}$:

$$\mathbf{D} \equiv -\frac{4\pi}{\Omega} \frac{\partial E}{\partial \mathbf{E}} = \frac{4\pi e}{\Omega} \sum_{s} \mathbf{Z}_s^{\star} \cdot \mathbf{u}_s + \boldsymbol{\epsilon}_{\infty} \mathbf{E}, \tag{42}$$

from which the macroscopic polarization, $\mathbf{P}$, is obtained via $\mathbf{D} = \mathbf{E} + 4\pi\mathbf{P}$. One finds the known result relating $Z^{\star}$ to the polarization induced by atomic displacements, at zero electric field:

$$Z_s^{\star\alpha\beta} = \frac{\Omega}{e} \left. \frac{\partial \mathbf{P}_{\alpha}}{\partial u_s^{\beta}(\mathbf{q}=0)} \right|_{\mathbf{E}=0}; \tag{43}$$

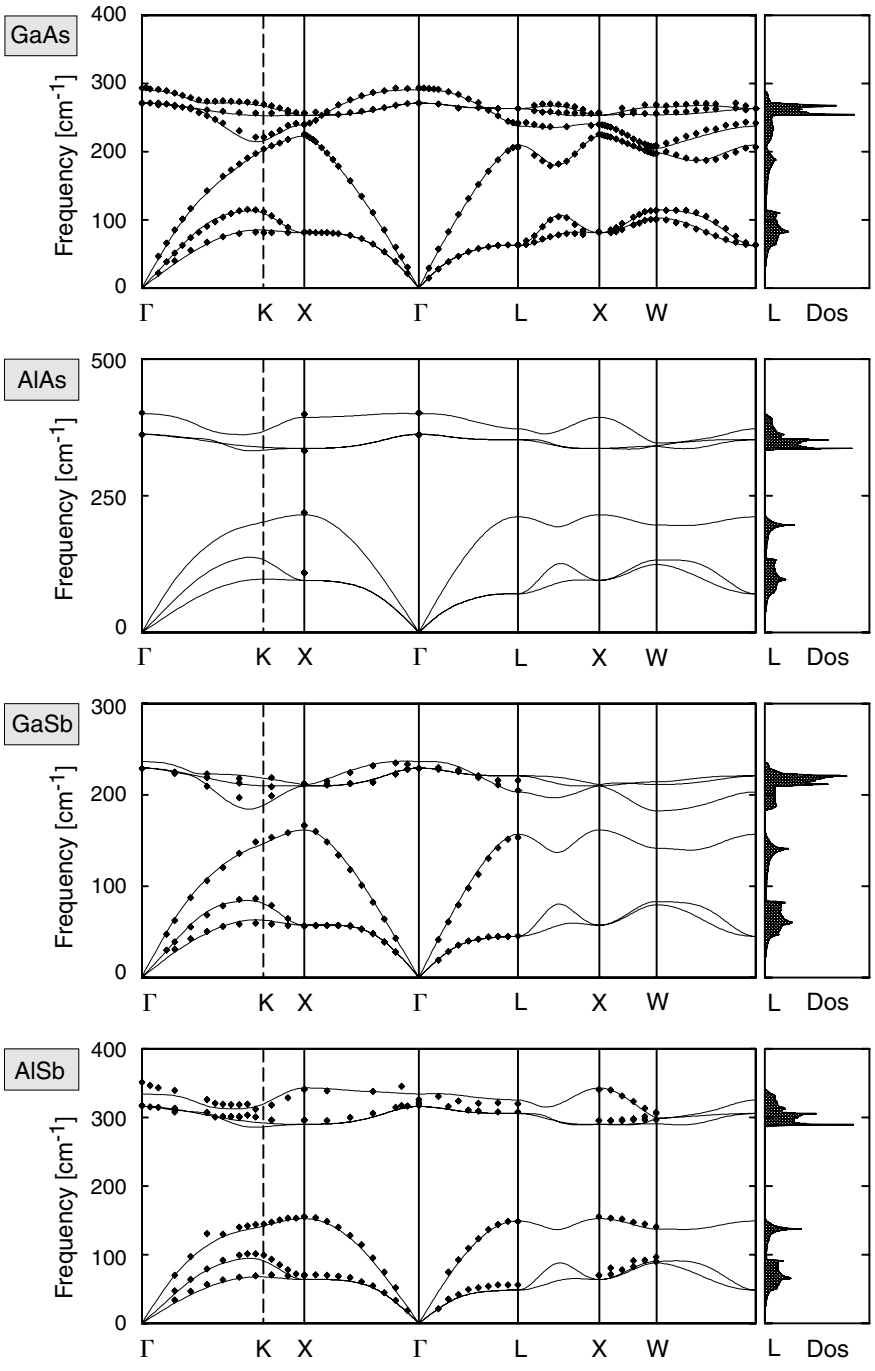

Figure 2. Calculated phonon dispersions and density of states for several III-V zincblende semiconductors. Experimental data are denoted by diamonds. Reproduced from Ref. [8].

while the electronic dielectric-constant tensor ϵ_∞ is the derivative of the polarization with respect to the macroscopic electric field at clamped nuclei:

$$\epsilon_\infty^{\alpha\beta} = \delta_{\alpha\beta} + 4\pi \left. \frac{\partial \mathbf{P}_\alpha}{\partial \mathsf{E}_\beta} \right|_{\mathbf{u}_s(\mathbf{q}=0)=0}. \tag{44}$$

DFPT provides an easy way to calculate $Z^\star$ and ϵ_∞ from first principles [8, 9]. The polarization linearly induced by an atomic displacement is given by the sum of an electronic plus an ionic term:

$$\frac{\partial \mathbf{P}_\alpha}{\partial u_s^\beta(\mathbf{q}=0)} = -\frac{e}{N_c\Omega} \int \mathbf{r} \frac{\partial n(\mathbf{r})}{\partial u_s(\mathbf{q}=0)} \mathrm{d}\mathbf{r} + \frac{e}{\Omega} Z_s \delta_{\alpha_\beta}. \tag{45}$$

This expression is ill-defined for an infinite crystal with Born–von Kármán periodic boundary conditions, because $\mathbf{r}$ is not a lattice-periodic operator. We remark, however, that we actually only need off-diagonal matrix elements $\langle \psi_m | \mathbf{r} | \psi_n \rangle$ with $m \neq n$ (see the discussion of Eqs. 20 and 21). These can be rewritten as matrix elements of a lattice-periodic operator, using the following trick:

$$\langle \psi_m | \mathbf{r} | \psi_n \rangle = \frac{\langle \psi_m | [H_{\mathrm{SCF}}, \mathbf{r}] | \psi_n \rangle}{\epsilon_m - \epsilon_n}, \quad \forall\, m \neq n. \tag{46}$$

The quantity $|\bar{\psi}_n^\alpha\rangle = r_\alpha |\psi_n\rangle$ is the solution of a linear system, analogous to Eq. (17):

$$(H_{\mathrm{SCF}} - \epsilon_n) |\bar{\psi}_n^\alpha\rangle = P_{\mathrm{c}} [H_{\mathrm{SCF}}, r_\alpha] |\psi_n\rangle, \tag{47}$$

where $P_{\mathrm{c}} = 1 - \sum_{n=1}^{N/2} |\psi_n\rangle\langle\psi_n|$ projects out the component over the occupied-state manifold. If the self-consistent potential acting on the electrons is local, the above commutator is simply proportional to the momentum operator:

$$[H_{\mathrm{SCF}}, \mathbf{r}] = -\frac{\hbar^2}{m} \frac{\partial}{\partial \mathbf{r}}. \tag{48}$$

Otherwise, the commutator will contain an explicit contribution from the nonlocal part of the potential [13]. The final expression for the effective charges reads:

$$Z_s^{\star\alpha\beta} = Z_s + \frac{4}{N_c} \sum_{n=1}^{N/2} \left\langle \bar{\psi}_n^\alpha \middle| \frac{\partial \psi_n}{\partial u_\beta(\mathbf{q}=0)} \right\rangle. \tag{49}$$

The calculation of ϵ_∞ requires the response of a crystal to an applied electric field $\mathbf{E}$. The latter is described by a potential, $V(\mathbf{r}) = e\mathbf{E}\cdot\mathbf{r}$, that is neither lattice-periodic nor bounded from below. In the linear-response regime,

however, we can use the same trick as in Eq. (46) and replace all the occurrences of $\mathbf{r}|\psi_n\rangle$ with $|\bar{\psi}_n^\alpha\rangle$ calculated as in Eq. (47). The simplest way to calculate ϵ_∞ is to keep the electric field $\mathbf{E}$ fixed and to iterate on the potential:

$$\frac{\partial V_{\rm SCF}(\mathbf{r})}{\partial \mathbf{E}} = \frac{\partial V(\mathbf{r})}{\partial \mathbf{E}} + \int \left(\frac{e^2}{|\mathbf{r}-\mathbf{r}'|} + \frac{\delta v_{\rm xc}(\mathbf{r})}{\delta n(\mathbf{r}')} \right) \frac{\partial n(\mathbf{r}')}{\partial \mathbf{E}} \mathrm{d}\mathbf{r}'. \tag{50}$$

One finally obtains:

$$\epsilon_\infty^{\alpha\beta} = \delta_{\alpha\beta} - \frac{16\pi e}{N_c \Omega} \sum_{n=1}^{N/2} \left\langle \bar{\psi}_n^\alpha \middle| \frac{\partial \psi_n}{\partial \mathsf{E}_\beta} \right\rangle. \tag{51}$$

Effective charges can also be calculated from the response to an electric field. In fact, they are also proportional to the force acting on an atom upon application of an electric field. Mathematically, this is simply a consequence of the fact that the effective charge can be seen as the second derivative of the energy with respect to an ion displacement and an applied electric field, and its value is obviously independent of the order of differentiation.

Alternative approaches – not using perturbation theory – to the calculation of effective charges and of dielectric tensors have been recently developed. Effective charges can be calculated as finite differences of the macroscopic polarization induced by atomic displacements, which in turn can be expressed in terms of a topological quantity – depending on the phase of ground-state orbitals – called the *Berry's phase* [10, 11]. When used at the same level of accuracy, the linear-response and Berry's phase approaches yield the same results. The calculation of the dielectric tensor using the same technique is possible by performing finite electric-field calculations (the electrical equivalent of the frozen-phonon approach). Recently, practical finite-field calculations have become possible [14, 15], using an expression of the position operator that is suitable for periodic systems.

5. Applications

The calculation of vibrational properties in the frozen-phonon approach can be performed using any methods that provide accurate forces on atoms. Localized basis-set implementations suffers from the problem of *Pulay forces*: the last term of Eq. (14) does not vanish if the basis set is incomplete. In order to obtain accurate forces, the Pulay term must be taken into account. The plane-wave (PW) basis set is instead free from such problem: the last term in Eq. (14) vanishes exactly even if the PW basis set is incomplete.

Practical implementations of DFPT equations is straightforward with PW's and norm-conserving pseudopotentials (PPs). In a PW-PP calculation, only valence electrons are explicitly accounted for, while the electron-ionic cores interactions are described by suitable atomic PPs. Norm-conserving PPs contain a nonlocal term of the form:

$$V^{\mathrm{NL}}_{\{\mathbf{R}\}}(\mathbf{r},\mathbf{r}') = \sum_{sl}\sum_{n,m} D_{nm}\beta^*_n(\mathbf{r}-\mathbf{R}_l-\boldsymbol{\tau}_s)\beta_m(\mathbf{r}'-\mathbf{R}_l-\boldsymbol{\tau}_s). \tag{52}$$

The nonlocal character of the PP requires some generalizations of the formulas described in the previous section, which are straightforward. More extensive modifications are necessary for "ultrasoft" PPs [16], which are appropriate to effectively deal with systems containing transition metal or other atoms that would otherwise require a very large PW basis set when using norm-conserving PPs. Implementations for other kinds of basis sets, such as LMTO, FLAPW, mixed basis sets (localized atomic-like functions plus PWs) exist as well.

Presently, phonon spectra can be calculated for materials described by unit cells or supercells containing up to several tens atoms. Calculations in simple semiconductors (Fig. 1 and 2) and metals (Fig. 3) are routinely performed with modest computer hardware. Systems that are well described by some flavor of DFT in terms of structural properties have a comparable accuracy in their phonon frequencies (with typical error in the order of a few percent points) and phonon-related quantities. The real interest of phonon calculations in simple systems, however, stems from the possibility to calculate real-space IFCs also in cases for which experimental data would not be sufficient to set up a reliable dynamical model (as, for instance, in AlAs, Fig. 2). The availability of IFCs in real space and thus of the complete phonon spectra allows for the accurate evaluation of thermal properties (such as thermal expansion coefficients in the quasi-harmonic approximation) and of electron–phonon coupling coefficients in metals.

Calculations in more complex materials are computationally more demanding, but still feasible for a number of nontrivial systems [2]: semiconductor superlattices and heterostructures, ferroelectrics, semiconductor surfaces [18], metal surfaces, high-T_c superconductors are just a few examples of systems successfully treated in the recent literature. A detailed knowledge of phonon spectra is crucial for the explanation of phonon-related phenomena such as structural phase transitions (under pressure or with temperature) driven by "soft phonons," pressure-induced amorphization, Kohn anomalies. Some examples of such phonon-related phenomenology are shown in Fig. 4–6. Figure 4 shows the onset of a phonon anomaly at an incommensurate $\mathbf{q}$-vector under pressure in ice XI, believed to be connected to the observed amorphization under pressure. Figure 5 displays a Kohn anomaly and the related lattice instability in the phonon spectra of ferromagnetic shape-memory alloy

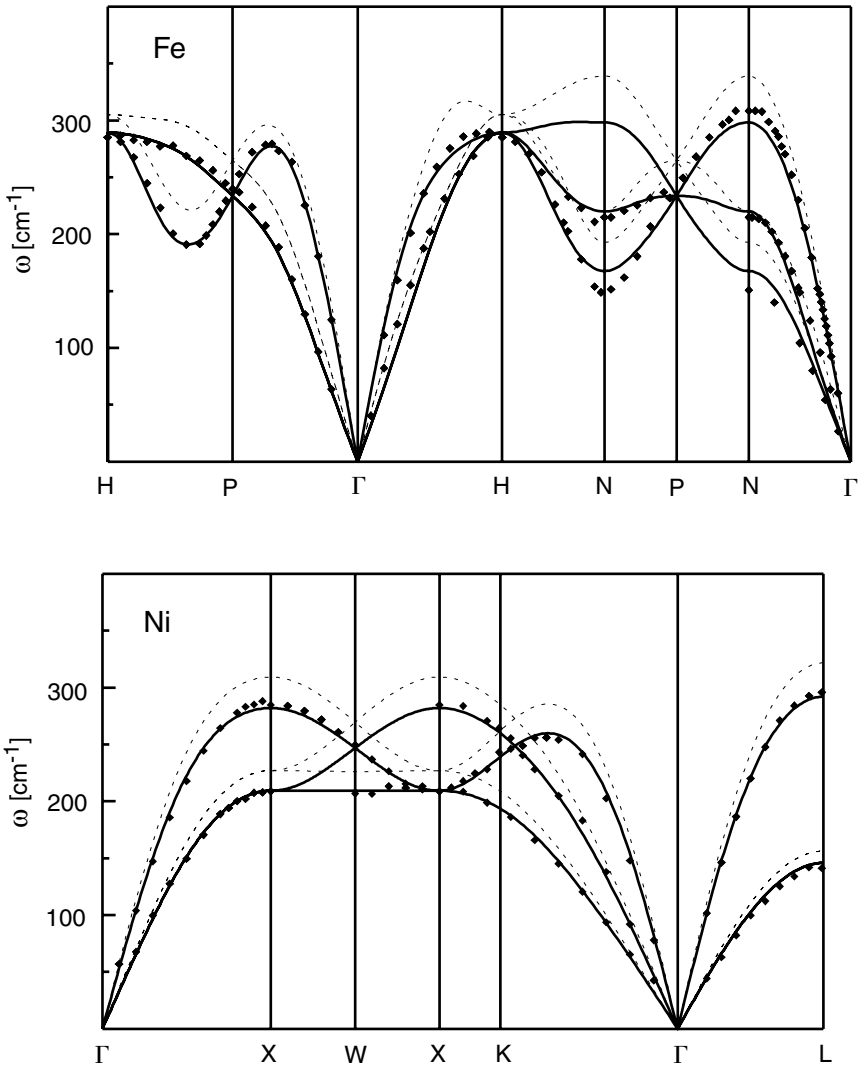

Figure 3. Calculated phonon dispersions, with spin-polarized GGA (solid lines) and LDA (dotted lines), for Ni in the face-centered cubic structure and Fe in the body-centered cubic structure. Experimental data are denoted by diamonds. Reproduced from Ref. [17].

Ni_2MnGa. Figure 6 shows a similar anomaly in the phonon spectra of the hydrogenated W(110) surface.

DFT-based methods can also be employed to determine Raman and infrared cross sections – very helpful quantities when analyzing experimental data. Infrared cross sections are proportional to the square of the polarization induced by a phonon mode. For the νth zone-center ($\mathbf{q} = 0$) mode,

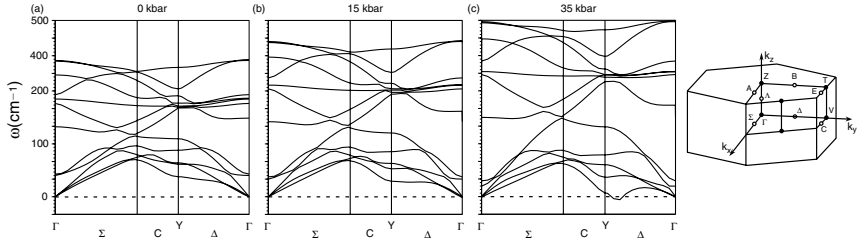

Figure 4. Phonon dispersions in ice XI at 0, 15, and 35 kbar. Reproduced from Ref. [19].

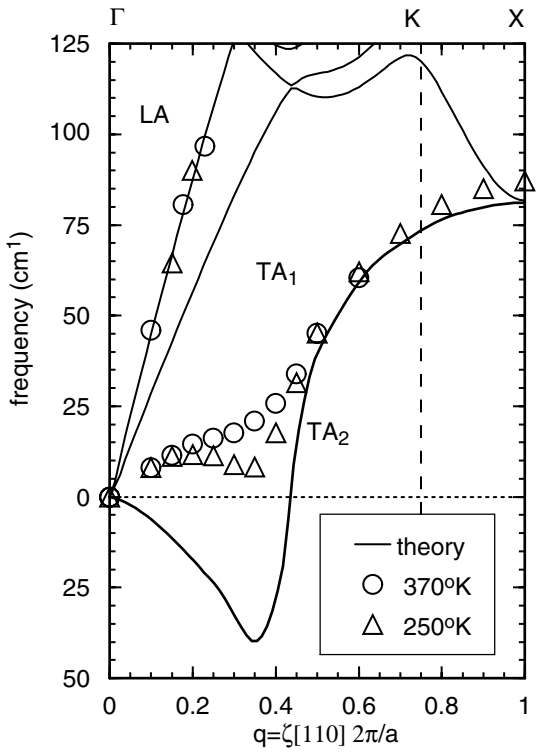

Figure 5. Calculated phonon dispersion of Ni_2MnGa in the fcc Heusler structure, along the $\Gamma - K - Z$ line in the [110] direction. Experimental data taken at 250 and 370 K are shown for comparison. Reproduced from Ref. [20].

characterized by a normalized vibrational eigenvector U_s^β, the oscillator strength f is given by

$$f = \sum_\alpha \left| \sum_{s\beta} Z^{\star\alpha\beta}_s U^\beta_s \right|^2 . \tag{53}$$

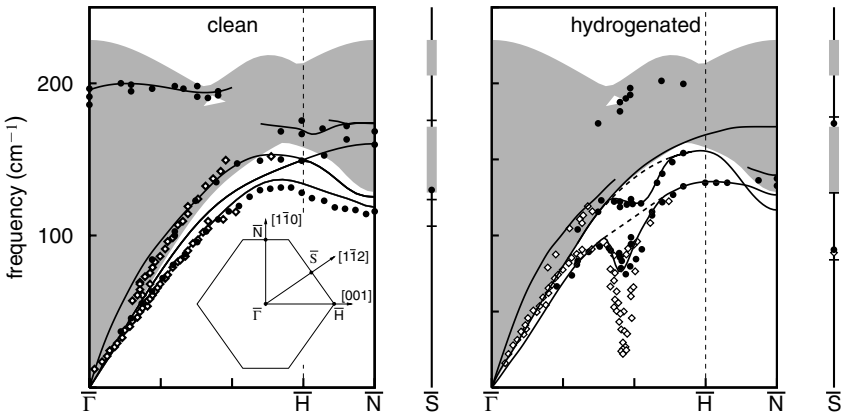

Figure 6. Phonon dispersions of the clean (left panel) and hydrogenated (right panel) W(110). Full dots indicate electron energy-loss data, open diamonds helium-atom scattering data. Reproduced from Ref. [21].

The calculation of Raman cross sections is difficult in resonance conditions, since the knowledge of excited-state Born–Oppenheimer surfaces is required. Off-resonance Raman cross sections are however simply related to the change of the dielectric constant induced by a phonon mode. If the frequency of the incident light, ω_i, is much smaller than the energy band gap, the contribution of the νth vibrational mode to the intensity of the light diffused in Stokes Raman scattering is:

$$I(\nu) \propto \frac{(\omega_i - \omega_\nu)^4}{\omega_\nu} r^{\alpha\beta}(\nu), \tag{54}$$

where α and β are the polarizations of the incoming and outgoing light beams, ω_ν is the frequency of the νth mode, and the *Raman tensor* $r^{\alpha\beta}(\nu)$ is defined as:

$$r^{\alpha\beta}(\nu) = \left\langle \left| \frac{\partial \chi^{\alpha\beta}}{\partial e_\nu} \right|^2 \right\rangle, \tag{55}$$

where $\boldsymbol{\chi} = (\epsilon_\infty - 1)/4\pi$ is the electric polarizability of the system, e_ν is the coordinate along the vibrational eigenvector U_s^β for mode ν, and $\langle\rangle$ indicates an average over all the modes degenerate with the νth one. The Raman tensor can be calculated as a finite difference of the dielectric tensor with a phonon frozen-in, or directly from higher-order perturbation theory [22].

6. Outlook

The field of lattice-dynamical calculations based on DFT, in particular in conjunction with perturbation theory, is ripe enough to allow a systematic application to systems and materials of increasing complexity. Among the most promising fields of application, we mention the characterization of materials through the prediction of the relation existing between their atomistic structure and experimentally detectable spectroscopic properties; the study of the structural (in)stability of materials at extreme pressure conditions; the prediction of the thermal dependence of different materials properties using the quasi-harmonic approximation; the prediction of superconductive properties via the calculation of electron–phonon coupling coefficients. We conclude mentioning that sophisticated open-source codes for lattice dynamical calculations [23] are freely available for download from the web.

References

[1] S. Baroni, P. Giannozzi, and A. Testa, "Green's-function approach to linear response in solids," *Phys. Rev. Lett.*, 58, 1861, 1987.
[2] S. Baroni, S. de Gironcoli, A. Dal Corso, and P. Giannozzi, etc. "Phonons and related crystal properties from density-functional perturbation theory," *Rev. Mod. Phys.*, 73, 515–562, 2001.
[3] X. Gonze, "Adiabatic density-functional perturbation theory," *Phys. Rev. A*, 52, 1096, 1995.
[4] J. Gerratt and I.M. Mills, *J. Chem. Phys.*, 49, 1719, 1968.
[5] R.D. Amos, In: K.P. Lawley (ed.), *Ab initio Methods in Quantum Chemistry – I*, Wiley, New York, p. 99, 1987.
[6] X. Gonze, "Perturbation expansion of variational principles at arbitrary order," *Phys. Rev. A*, 52, 1086, 1995.
[7] X. Gonze, "First-principles responses of solids to atomic displacements and homogeneous electric fields: Implementation of a conjugate-gradient algorithm," *Phys. Rev. B*, 55, 10337, 1997.
[8] P. Giannozzi, S. de Gironcoli, P. Pavone, and S. Baroni, "*Ab initio* calculation of phonon dispersions in semiconductors," *Phys. Rev. B*, 43, 7231, 1991.
[9] X. Gonze and C. Lee, "Dynamical matrices, Born effective charges, dielectric permittivity tensors, and interatomic force constants from density-functional perturbation theory," *Phys. Rev. B*, 55, 10355, 1997.
[10] D. Vanderbilt and R.D. King-Smith, "Electric polarization as a bulk quantity and its relation to surface charge," *Phys. Rev. B*, 48, 4442, 1993.
[11] R. Resta, "Macroscopic polarization in crystalline dielectrics: the geometrical phase approach," *Rev. Mod. Phys.*, 66, 899, 1994.
[12] M. Born and K. Huang, *Dynamical Theory of Crystal Lattices.*, Oxford University Press, Oxford, 1954.
[13] S. Baroni and R. Resta, "*Ab initio* calculation of the macroscopic dielectric constant in silicon," *Phys. Rev. B*, 33, 7017, 1986.

[14] P. Umari and A. Pasquarello, "*Ab initio* molecular dynamics in a finite homogeneous electric field," *Phys. Rev. Lett.*, 89, 157602, 2002.
[15] I. Souza, J. Íñiguez, and D. Vanderbilt, "First-principles approach to insulators in finite electric fields," *Phys. Rev. Lett.*, 89, 117602, 2002.
[16] D. Vanderbilt, "Soft self-consistent pseudopotentials in a generalized eigenvalue formalism," *Phys. Rev. B*, 41, 7892, 1990.
[17] A. Dal Corso and S. de Gironcoli, "Density-functional perturbation theory for lattice dynamics with ultrasoft pseudo-potentials," *Phys. Rev. B*, 62, 273, 2000.
[18] J. Fritsch and U. Schröder, "Density-functional calculation of semiconductor surface phonons," *Phys. Rep.*, 309, 209–331, 1999.
[19] K. Umemoto, R.M. Wentzcovitch, S. Baroni, and S. de Gironcoli, "Anomalous pressure-induced transition(s) in ice XI," *Phys. Rev. Lett.*, 92, 105502, 2004.
[20] C. Bungaro, K.M. Rabe, and A. Dal Corso, "First-principle study of lattice instabilities in ferromagnetic Ni_2MnGa," *Phys. Rev. B*, 68, 134104, 2003.
[21] C. Bungaro, S. de Gironcoli, and S. Baroni, "Theory of the anomalous Rayleigh dispersion at H/W(110) surfaces," *Phys. Rev. Lett.*, 77, 2491, 1996.
[22] M. Lazzeri and F. Mauri, "High-order density-matrix perturbation theory," *Phys. Rev. B*, 68, 161101, 2003.
[23] PWscf package: www.pwscf.org. ABINIT: www.abinit.org.